Eur Biophys J (1987) 14: 179–193

European Biophysics Journal

Depolarized fluorescence photobleaching recovery

R. E. Dale

Paterson Institute for Cancer Research, Christie Hospital & Holt Radium Institute, Manchester M20 9BX, UK

Received November 11, 1985/Accepted in revised form July 7, 1986

Abstract. The effects of the fact that the laser sources typically used in fluorescence photobleaching recovery (FPR) experiments in the most commonly employed in-line microscope imaging geometries, are highly linearly polarized, are examined in some detail. The implications of the results, in particular for the interpretation of FPR data in complex cell membrane systems in terms of laterally mobile and immobile sub-populations of the labelled molecular species of concern, are discussed. Methods of experimentally eliminating the potentially major rotational diffusion-based "artifacts", different from those appropriate to three-dimensional (solution or suspension) systems which require other than in-line geometries, are delineated.

Key words: FPR, FRAP, translational and rotational diffusion, membranes, supramolecular assembly

Introduction

In the decade or so since its effective inception (Yguerabide 1971; Peters et al. 1974; Edidin et al. 1976; Jacobson et al. 1976a, b; Zagyansky and Edidin 1976; Axelrod et al. 1976; Schlessinger et al. 1976) the technique of *fluorescence photobleaching recovery* (FPR), alternatively widely known as *fluorescence recovery after photobleaching* (FRAP) or as *fluorescence microphotolysis,* has been widely adopted for the measurement of translational diffusion of both small fluorophoric reporter molecules and fluorescently labelled proteins in a variety of biological systems. Both lateral diffusion in the membranes and translational diffusion in the cytoplasm of living cells or organelles, as well as in relatively simple model membrane and isolated protein assembly systems respectively, have been extensively studied. The theory, practice in a variety of forms, mainly "spot", but also "periodic pattern" (Smith and McConnell 1978) photobleaching, various artifacts that might particularly arise from the use of laser light sources such as "local heating" and photochemical damage and, for the membrane experiments, interpretation of the results in terms of the "fluid mosaic membrane" hypothesis (Singer and Nicolson 1972), have been considered in some depth in a number of recent review articles on FPR in model and/or living cell membranes (Bretscher 1980; Flanagan 1980; Jacobson 1980; Edidin 1981; Jacobson and Wojcieszyn 1981; Peters 1981; Webb 1981; Jacobson et al. 1982; Vaz et al. 1982; Jacobson 1983; Koppel 1983; Hoffmann and Restall 1983; Barisas 1984; Axelrod 1985) and cytoplasm (Ware 1985). The implications of FPR data on lateral diffusion in model membranes for a qualitative description of the situation in biological membranes have also been examined recently in terms of different models of diffusion in such systems (Vaz et al. 1984, 1985). The importance of good quantitative estimates of lateral diffusion coefficients in biological membranes to an understanding of cell function, and possible dysfunction in pathological cell states, has been clearly and succinctly indicated by Bretscher (1980), and the paradoxical relationship between FPR and other physically based estimates of lateral diffusion coefficients and those arrived at indirectly from membrane biochemical considerations discussed (Kell 1984; O'Shea 1984, 1985; Pink 1985; Kaprelyants 1985).

Theoretical expectations based on fluid hydrodynamic considerations (Saffman and Delbrück 1975; Saffman 1976; Hughes et al. 1981, 1982) appeared initially to be well realized in the results of FPR measurements of the lateral diffusion coefficients of both small molecules and of mono- or

Abbreviations: FPR, fluorescence photobleaching recovery; FRAP, fluorescence recovery after photobleaching; 2- and 3-D, two- and three-dimensional

pauci-meric (unaggregated) proteins in *model* membrane systems – $D \sim 5 \times 10^{-8} - 5 \times 10^{-9}\,cm^2\,s^{-1}$ (Jacobson and Wojcieszyn 1981; Peters and Cherry 1982). Recent, more detailed examination of small molecule FPR, however, has provided results inconsistent with the above, but interpretable on the basis of a "free volume" ("free area") model of diffusion (Vaz and Hallmann 1983; Vaz et al. 1984, 1985). For cell membranes, however, while the small molecules tend to diffuse at very similar rates, the majority of proteins that diffuse do so very much more slowly – by one to four orders of magnitude (Jacobson and Wojcieszyn 1981), and there is typically a large fraction of protein that appears to be *immobile* ($D \lesssim 3 \times 10^{-12}\,cm^2\,s^{-1}$). A schematic of a typical (idealized) experimental result is shown in Fig. 1. Furthermore, FPR due to directed flow rather than diffusion must also be considered in living cell membranes (Axelrod et al. 1976; Koppel 1979; van Zoelen et al. 1983). In addition, there are many possibilities for further complexity to arise in such systems which may be characterized by high degrees of heterogeneity, asymmetry and non-planarity, over the relatively large characteristic dimension of the spot or pattern period, some of which have been dealt with at least from a theoretical viewpoint (Smith et al. 1979; Owicki and McConnell 1980; Aizenbud and Gershon 1982; Wolf et al. 1982).

A particularly elegant method of obtaining lateral diffusion coefficients for small membrane probes oriented in spherical bilayer membranes (vesicles) utilises the fact that the laser bleaching and monitoring source is *linearly polarized* (Smith et al. 1981 a). The whole vesicle is illuminated and the observed recovery has an exponential component reflecting *reorientational* randomization of the probe as it diffuses around the curved vesicle surface. The polarization of the laser source was subsequently also utilised in measurements of slow *rotational* diffusion of probes in both vesicles and planar model membranes in which lateral diffusion was negligibly small (Smith et al. 1981 b), estimated directly from polarized recovery and depletion signals, and in cell membranes (Johnson and Garland 1981) by "depolarization of fluorescence depletion".

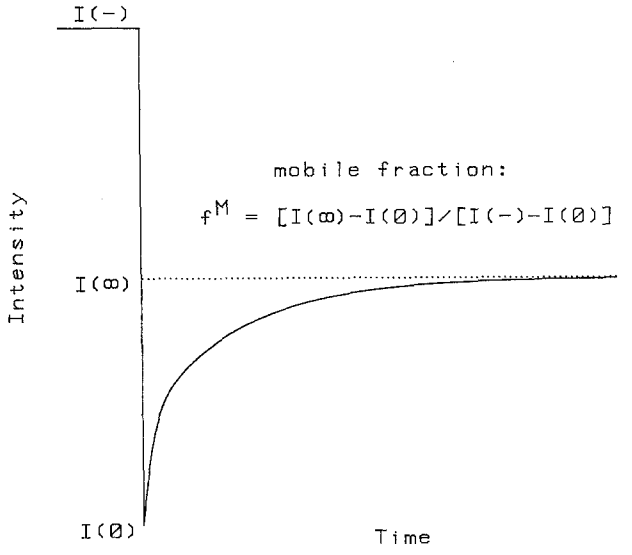

Fig. 1. Schematic of typical fluorescence photobleaching recovery curve exhibiting low initial level after bleaching at time zero, and partial recovery to a steady level lower than the pre-bleach one indicative of immobility of some of the bleached material

These results imply a potential rotational diffusion artifact in lateral diffusion measurements by FPR, since the polarization of the laser bleaching and monitoring beam is generally uncontrolled but high, e.g. > 95% at the sample after passage through the focussing microscope objective (Smith et al. 1981 b). As has recently been pointed out (Wegener and Rigler 1984), while rotational diffusion of a single, non-interacting species is very much faster than lateral diffusion, so that all rotational artifacts are averaged out on the time-scale of measurement of the latter, the time-scales for different components in a heterogeneous system may overlap. The direct measurement of either process will then potentially be subject to interference by the other. The possibility of interference in lateral diffusion FPR measurements of rotational diffusion on a commensurate time scale had actually already been pointed out (Tait and Frieden 1982), but not quantitated in any way, for solution FPR. Wegener and Rigler examined this case in detail and showed that, if the emission monitored is unbiased with respect to its direction and polarization, a condition attained by collection over 2π (or 4π) steradians (Wegener and Rigler 1984) or, for certain beam geometries, by the summation of appropriately weighted polarized components of emission (Wegener 1984), any possible rotational artifact will be eliminated if the polarizations of bleaching and monitoring excitation beams are set up at the well-known "magic angle" of $\sim 55°$, obtained from the condition that the second order Legendre polynomial

$$P_2(\cos\psi) = (3/2)\cos^2\psi - (1/2)\,,$$

where ψ is the angle between the electric vectors of the two polarized beams, disappears. Actually, the necessity for this "magic angle" condition had effectively already been realized almost a decade earlier (Lessing et al. 1975; Lessing and von Jena 1976, 1979) in connection with picosecond laser transient absorption experiments – FPR is essentially equivalent to fluorescence-monitored transient absorption

– although there it is the "contamination" of level kinetics by depolarization that is of concern.

More recently, it has been pointed out that similar, but quantitatively different, considerations apply to the two-dimensional (oriented membrane) FPR experiment, and the effect of this on the interpretation of existing FPR data for cell membrane systems, particularly in regard to quantitation of the fraction of labelled species that is diffusing laterally and its absolute coefficient, discussed briefly (Dale 1985). In the present contribution, this result is derived in full under the simplifying assumptions made there, and is extended to include some consideration of the effects of selection of polarized components of emission and to relax some of the more stringent simplifying conditions to those which more nearly obtain in a typical FPR experiment. The three-dimensional case (Wegener and Rigler 1984; Wegener 1984) is similarly considered for comparison, the implications of these results for the experimental determination of lateral diffusion characteristics by FPR discussed, and protocols for checking polarization effects and eliminating them in the 2- and 3-dimensional situations emphasized.

Theory

To illustrate the extent to which rotational diffusion may affect the determination of the parameters of translational diffusion by the FPR method in both 2- and 3-dimensional systems, the time-course of recovery (or depletion) resulting from rotational diffusion alone, in the complete absence of translational diffusion or flow, following bleaching induced by a polarized source, will be examined first under idealized conditions. These are, nevertheless, approached quite closely in the majority of FPR experiments, at least in the biological and biochemical spheres of interest, which typically utilize laser light sources delivered *via* a microscope optical system for bleaching and monitoring (e.g. Koppel et al. 1976; Koppel 1983; Barisas 1984). The initial idealizing assumptions are:

(i) the bleachable fluorophore is representable as bearing perfectly linear absorption and emission transition moments which are also colinear (or parallel) and are fixed rigidly in the framework of the rotating species considered;

(ii) the bleaching and monitoring laser beams are (a) perfectly linearly polarized, (b) perfectly colinear, and (c) in the case in which the sample under investigation is 2-dimensional, fall perpendicularly onto its perfectly planar surface;

(iii) the observed fluorescence induced by the monitoring beam is (a) also perfectly colinear with it, and (b) of an intensity representative of the *total* emission in this direction, i.e. unbiased with respect to its polarization;

(iv) the bleaching pulse is of very short duration compared with the relaxation times of interest (δ-pulse);

(v) the elementary bleaching process for fluorophores in a given orientation with respect to the electric vector of a section of the bleaching beam of given uniform intensity is (a) exponential with time during the bleaching period, i.e. a constant (large) fraction of the fluorophores are in the excited state during this time, and (b) irreversible;

(vi) the monitoring beam is of low enough intensity that (a) further bleaching during the monitoring period is negligible, and (b) no non-linear (coherence) effects are observable;

(vii) while the rotational motions considered may arise from one or more species, and may be isotropic or anisotropic in the 3-dimensional case, e.g. for a solution of macromolecular aggregates or a suspension of membrane vesicles, the only mode of rotation occurring in the 2-dimensional case is uniaxial about the normal to the plane.

As will be indicated, the relaxation of some of these assumptions that is required to approximate somewhat better the physical realities of typical FPR experiments, related both to ideality of the probe and the optical system, generally only require simple, though sometimes tedious, additional work. These will be examined separately in order not to obscure the development of the basic results. For this purpose also, the normal condition in FPR that the bleaching and monitoring laser beams are identical except with respect to their intensity, specifically that their planes of polarization are identical, will be relaxed.

The 2-dimensional case

Consider first the relevant geometry for the static situation depicted in Fig. 2. The vector $\boldsymbol{e}$ represents the projection of the absorption-emission transition moment $\boldsymbol{E}$ which makes an angle θ with the direction of light propagation, i.e. with the normal $\boldsymbol{n}$ to the plane depicted. The latter contains also the electric vectors $\boldsymbol{B}$ and $\boldsymbol{M}$ of the linearly polarized bleaching and monitoring beams at the moment of excitation with which $\boldsymbol{e}$ subtends angles α and β respectively, ψ being the angle between them.

Before bleaching, the intensity of emission observed along $\boldsymbol{n}$ is proportional to the probabilities of absorption ($\sin^2\theta \cos^2\beta$) and emission ($\sin^2\theta$) at the angular coordinates (θ, β) in the interval $d\beta$, so that the overall pre-bleach intensity observed is given by:

$$I(-) = C \sin^4\theta \int_{\beta=0}^{\pi} \cos^2\beta \, d\beta = \pi C \sin^4\theta/2 \,, \qquad (1)$$

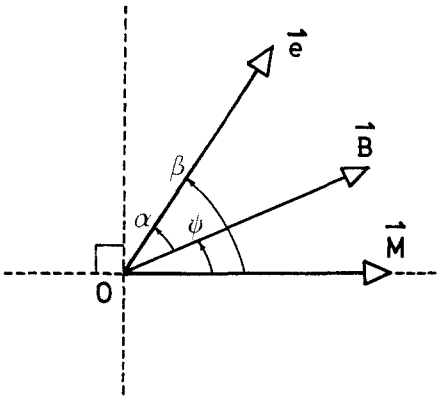

Fig. 2. Schematic of the angular relationships of electric vectors of bleaching and monitoring beams (***B*** and ***M*** respectively) and the projection (***e***) onto the membrane plane of the absorption/emission transition moment (***E***) of the bleachable probe attached to a membrane constituent (e.g. protein) or otherwise adsorbed into the membrane

where C is an angle-independent constant including the intensity of the monitoring beam, extinction coefficient of the fluorophore at the excitation wavelength and the quantum yield of fluorophore emission. The intensity observed after the bleach will be proportional also to the probability that fluorophores at coordinates (θ, β) were not bleached, which may be expressed in terms of a "bleaching parameter" B proportional to the intensity and duration of the bleaching "pulse" and to the absorption coefficient and intrinsic molecular bleaching efficiency. For a beam section of uniform intensity this probability is given by:

$$P(B,\alpha) = \exp[-B\cos^2\alpha] \tag{2}$$

while for a beam of gaussian radial intensity distribution it is described by the confluent hypergeometric function:

$$P(B,\alpha) = (1-\exp[-B\cos^2\alpha])/B\cos^2\alpha\,. \tag{3}$$

The "polarized" bleaching parameter B is related to the originally defined "unpolarized" bleaching parameter K (Axelrod et al. 1976; Jacobson et al. 1976a) by $K = B/2$ for this case, the factor of 2 taking into account the average value for random orientation in two dimensions:

$$\langle\cos^2\alpha\rangle = \int_{\alpha=0}^{\pi}\cos^2\alpha\,d\alpha \Big/ \int_{\alpha=0}^{\pi} d\alpha = 1/2\,, \tag{4}$$

which appears implicitly in K. Both bleaching parameters also contain the geometrical factor $\sin^2\theta$ incorporated implicitly into the effective extinction coefficient. Thus, immediately after the bleach:

$$I_\psi = C\sin^4\theta \int_{\beta=0}^{\pi}\cos^2\beta\,P(B,\alpha)\,d\beta \tag{5}$$

the subscript ψ indicating that the angular dependence, after integration over β and therefore also α, will reside only in the difference, $\psi = \beta - \alpha$.

Similarly, the evolution of intensity with time after the δ-pulse bleach, $I_\psi(t)$, is given by Eq. (5) with $\beta(t)$ for β. If this is due to unrestricted uniaxial Brownian rotation, as explicitly considered here, the evolution of $\overline{\cos^2\beta(t)}$, where the bar is included to signify that this is a time- and ensemble-average, is described for a single rotating species by:

$$2\overline{\cos^2\beta(t)} - 1 = (2\cos^2\beta - 1)\exp[-4D_\parallel t]\,, \tag{6}$$

where $D_\parallel$ is the uniaxial rotational diffusion coefficient (Weber 1953). On combining Eqs. (1) and (6) with the time-dependent analogue of Eq. (5), and substituting $\beta = \psi + \alpha$, $d\beta = d\alpha$, a normalised time-course $F_\psi(t)$ may be defined:

$$\begin{aligned} F_\psi(t) &= I_\psi(t)/I(-) \\ &= (1/\pi)\int_{\alpha=-\psi}^{\pi-\psi}\{1+[2\cos^2(\psi+\alpha)-1]\exp[-4D_\parallel t]\} \\ &\qquad \cdot P(B,\alpha)\,d\alpha\,. \end{aligned} \tag{7}$$

This is usefully rewritten as:

$$F_\psi(t) = \{F_\psi(0) - F(\infty)\}\exp[-4D_\parallel t] + F(\infty)\,, \tag{8}$$

where:

$$\begin{aligned} F_\psi(0) &= (2/\pi)\int_{\alpha=0}^{\pi}\cos^2(\psi+\alpha)\,P(B,\alpha)\,d\alpha \\ &= (4/\pi)\int_{\alpha=0}^{\pi/2}\cos^2(\psi+\alpha)\,P(B,\alpha)\,d\alpha \end{aligned} \tag{9}$$

and similarly:

$$F(\infty) = (2/\pi)\int_{\alpha=0}^{\pi/2} P(B,\alpha)\,d\alpha \tag{10}$$

the convenient compact integral forms being valid in the case of the kinds of bleaching probability functions considered, i.e. for $P(B,\alpha) \equiv P(B,\cos^2\alpha)$ [see Eqs. (2) and (3)], the subscript for $F(\infty)$ being omitted to indicate its independence of ψ.

Equation (9) may also, after expanding the $(\psi+\alpha)$ cosine square and dropping the cross-term whose product with $P(B,\alpha)$ will disappear over the half-cycle of integration, be usefully expressed in the forms:

$$F_\psi(0) = \cos^2\psi\,F_\parallel(0) + \sin^2\psi\,F_\perp(0) \tag{11}$$

and

$$\begin{aligned} F_\psi(0) &= 2\cos^2\psi\,F(\infty) - (2\cos^2\psi - 1)\,F_\perp(0) \\ &= (2\cos^2\psi - 1)\,F_\parallel(0) + 2\sin^2\psi\,F(\infty)\,, \end{aligned} \tag{12}$$

where:

$$F_\parallel(0)\,[=F_0(0)] = (4/\pi)\int_{\alpha=0}^{\pi/2}\cos^2\alpha\,P(B,\alpha)\,d\alpha \tag{13}$$

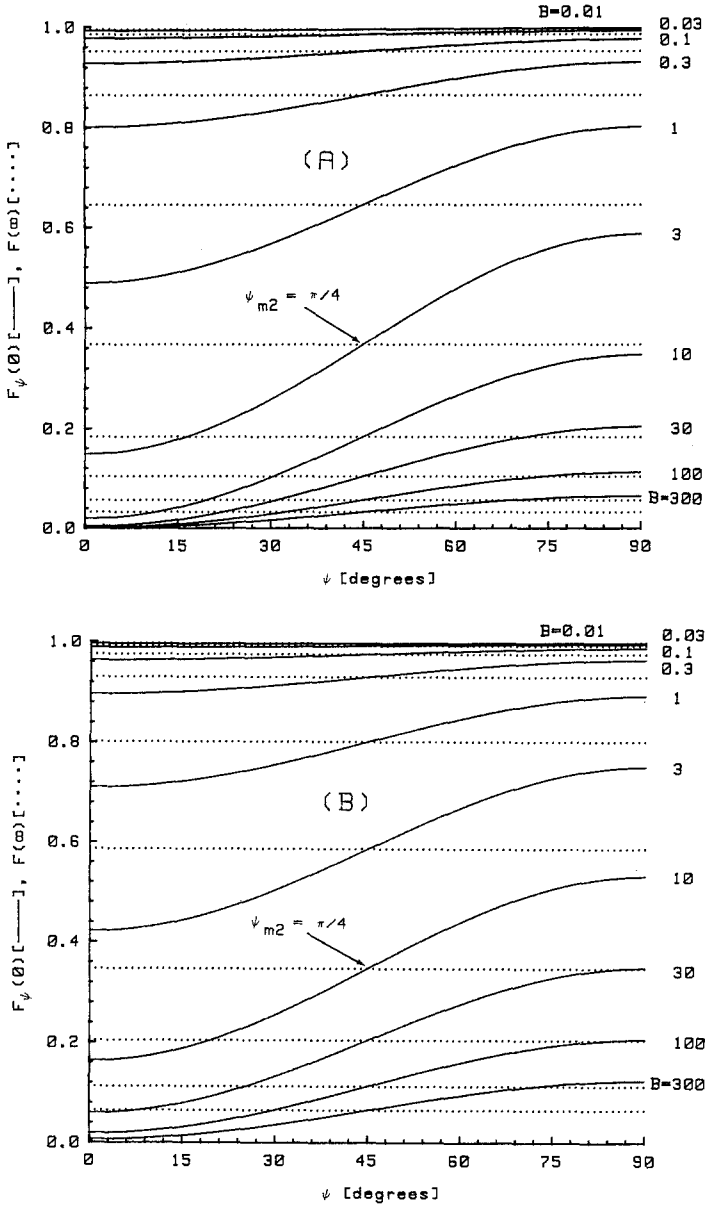

Fig. 3A and B. Variation of initial and final levels of fluorescence intensity monitored following a bleaching pulse, relative to unit pre-bleach intensity (cf. Fig. 1), $F_\psi(0)$ and $F(\infty)$, as a function of the angle ψ between the electric vectors of bleaching and monitoring beams (cf. Fig. 2), for different values of the bleaching parameter B in the idealized cases of (**A**) spatially uniform and (**B**) gaussian cross-sectional laser beam intensity profiles (Axelrod et al. 1976) for 2-dimensional FPR in the rotationally mobile, laterally immobile limit. Recovery occurs for $0 \leqq \psi < \pi/4$, depletion for $\pi/4 < \psi \leqq \pi/2$. No rotational effect is apparent at the "magic angle" $\psi = \psi_{m2} = \pi/4$ for which $F_\psi(0) = F_\psi(t) = F(\infty)$

and

$$F_\perp(0)\,[=F_{\pi/2}(0)] = (4/\pi)\int_{\alpha=0}^{\pi/2} \sin^2\alpha\, P(B,\alpha)\, d\alpha\,. \qquad (14)$$

On substituting Eq. (12) into Eq. (8) it is also seen that:

$$\begin{aligned} F_\psi(t) &= (2\cos^2\psi - 1)\,\{F(\infty) - F_\perp(0)\}\cdot \exp\,[-4D_\parallel t] \\ &\quad + F(\infty) \\ &= (2\cos^2\psi - 1)\,\{F_\parallel(0) - F(\infty)\}\cdot \exp\,[-4D_\parallel t] \\ &\quad + F(\infty)\,. \end{aligned} \qquad (15)$$

From these expressions it is readily evident that:

$$F_{\pi/4}(t) = F_{\pi/4}(0) = [F_\parallel(0) + F_\perp(0)]/2 = F(\infty) \qquad (16)$$

as depicted in Fig. 3 which illustrates the dependence of $F_\psi(0)$ on the bleaching parameter B. The dependence of $F_\parallel(0)$ and $F(\infty)$ on the bleaching parameter are shown in Fig. 4, the former corresponding to the (idealized) heretofore normal experimental situation for FPR determinations using a laser for bleaching and monitoring, the latter to an experimental protocol which would eliminate the influence of slow rotational motion on the observed signal.

Since the effects predicted by Eq. (15) result from a rotational motion which gives rise to depolarization, it is no surprise that they may be simply re-expressed in terms of Jabłoński's emission anisotropy (Jabłoński 1960), $r(t)$ which, for the two-dimensional case considered here, equates formally with the more classically defined polarization $p(t)$:

$$F_\psi(t) = F(\infty) - (2\cos^2\psi - 1)\,[1 - F(\infty)]\,p(t) \qquad (17)$$

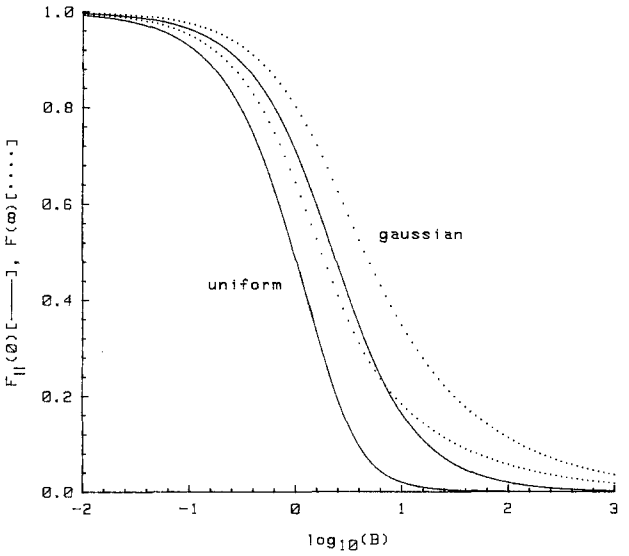

Fig. 4. Change of inital and final levels of fluorescence intensity monitored following a bleaching pulse, relative to unit prebleach intensity, $F_{\parallel}(0)$ for $\psi = 0$, i.e. electric vectors of bleaching and monitoring beams parallel, and $F(\infty)$, respectively as a function of the bleach parameter B in the idealized cases of uniform *(lower-pair)* and gaussian *(upper pair)* beam intensity profiles, for 2-D FPR in the rotationally mobile, laterally immobile limit

as previously presented elsewhere without proof (Dale 1985), where p, the "polarization of fluorescence depletion" (Johnson and Garland 1981) is defined by:

$$p = \{F'_{\parallel} - F'_{\perp}\}/\{F'_{\parallel} + F'_{\perp}\}\,; \quad F' = 1 - F \tag{18}$$

or in the alternative forms:

$$\begin{aligned} p &= \{F'_{\parallel} - F'_{\perp}\}/2F'(\infty) \\ &= \{F'_{\parallel} - F'(\infty)\}/F'(\infty) \\ &= \{F'(\infty) - F'_{\perp}\}/F'(\infty) \end{aligned} \tag{19}$$

while:

$$p(t) = p_0 \exp[-4D_{\parallel} t]\,, \tag{20}$$

where p_0 is the zero-point polarization. Further, if the result expressed in Eq. (8) for $0 \leqq \psi < \pi/4$ were to be interpreted as though it represented recovery via lateral diffusion, the recovery to $F(\infty) < 1$ would correspond to an apparently laterally mobile fraction f_{ψ}^{M}, given by:

$$f_{\psi}^{M} = \{F(\infty) - F_{\psi}(0)\}/\{1 - F_{\psi}(0)\} \tag{21}$$

which again is simply related to the zero-point polarization via the limit of Eq. (17) for $t = 0$. In particular, for $\psi = 0$:

$$f_{\parallel}^{M} = p_0/(1 + p_0)\,, \tag{22}$$

while for $\psi = \pi/4$ it disappears, and in $\pi/4 < \psi \leqq \pi/2$ it becomes negative, signalling its "artifactual" origin. f_{ψ}^{M} is shown as a function of the bleaching parameter in Fig. 5, while the dependences of $f_{\parallel}^{M}$ and p_0 on B are depicted in Fig. 6. As evident there, the low bleach limits, given exactly by expanding the exponential in $P(B,\alpha)$ and performing the integrations of e.g. Eqs. (10) and (13) analytically, are $f_{\parallel}^{M}(B \to 0) = 1/3$, $p_0(B \to 0) = 1/2$ for both uniform and gaussian beams, while in the high bleach limit, $f_{\parallel}^{M}(B \to \infty) = p_0(B \to \infty) = 0$.

It is thus clear that, if an FPR signal free of the effects of possible slow rotational motions is to be registered under the idealized conditions envisaged here, the planes of linearly polarized bleaching and monitoring beams should be oriented at the 2-D "magic angle" $\psi_{m2} = \cos^{-1}\sqrt{1/2} = 45°$ to each other. This may readily be accomplished in practice by insertion of a polarizing element in the beam path, either a polarizer which may be reoriented through $\pi/4$ radians or a half-wave plate with orientations adjustable by $\pi/8$. While the provision of such elements would also allow access to rotational phenomena, if it is only lateral diffusion that is of concern, the equivalent condition may be attained by insertion of a depolarizing element, either an appropriately oriented quarter-wave plate or scrambling wedge, into the beam path. The condition that emission intensity be registered without bias as to its polarization may likewise be ensured by insertion of a similar depolarizer in the observation path. These may of course constitute physically the same depolarizer in the common beam path.

It is also of some interest to examine the effects that observation of a particularly polarized emission component elicit (compare Smith et al. 1981 b). This geometry is depicted in Fig. 7. In the stationary situation, $\boldsymbol{E}$ subtends an angle γ with $\mathbf{0}$, the electric vector of the emission selected by a (perfect) polarizer whose transmission vector is oriented at an angle ω to the electric vector of the monitoring beam. The before-bleach intensity monitored is then given by:

$$I_{\omega}(-) = C \sin^4\theta \int_{\beta=0}^{\pi} \cos^2\beta \cos^2\gamma \, d\beta\,, \tag{23}$$

where $\gamma = \beta - \omega$ so that, after expansion of $\cos^2\gamma$, integration and collection of terms:

$$I_{\omega}(-) = \pi C \sin^4\theta\,(2\cos^2\omega + 1)/8\,. \tag{24}$$

Similarly, on expanding $\cos^2\gamma$, $\cos^2\alpha$ and the exponential appearing in $P(B,\alpha)$ according to Eqs. (2) or (3) and collecting terms, the time-dependence

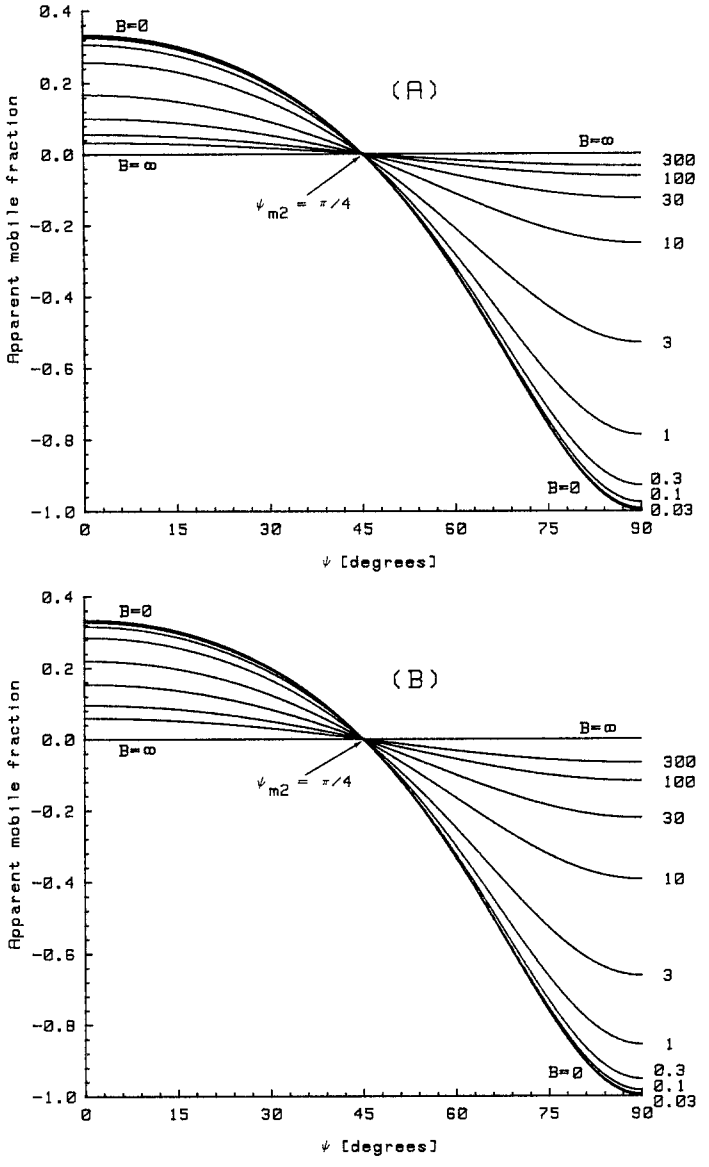

Fig. 5A and B. Variation of the apparent laterally mobile fraction f_{ψ}^{M} [cf. Fig. 1 and Eq. (21)] artifactually resulting, in the absence of detectable lateral diffusion, from uniaxial rotation of the bleachable label in 2-D FPR measurements in the idealized cases of (**A**) uniform and (**B**) gaussian beam intensity profiles. The negative values observed for $\pi/4 < \psi \leqq \pi/2$ correspond to a depletion of signal under these conditions rather than recovery, and are diagnostic of its "artifactual" origin. The artifact disappears at the "magic angle" $\psi_{m2} = 45°$ for which:

$f_{\psi_{m2}}^{M} = 0$

at all bleaching ratios

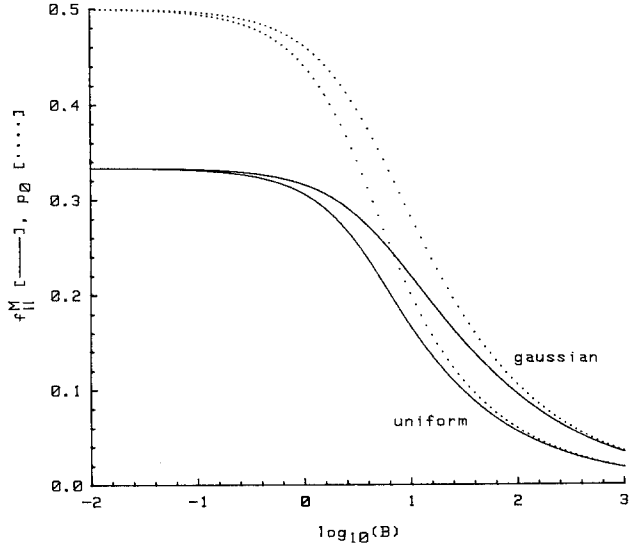

Fig. 6. Change of apparent mobile fraction $f_{\parallel}^{M}$ observed for $\psi = 0$ (electric vectors of bleaching and monitoring beams parallel) and of p_0, the zero-point polarization to which $f_{\parallel}^{M}$ is related by Eq. (22), as a function of the bleaching parameter B for 2-D FPR in the rotationally mobile, laterally immobile limit in the idealized cases of uniform *(lower pair)* and gaussian *(upper pair)* beam intensity profiles

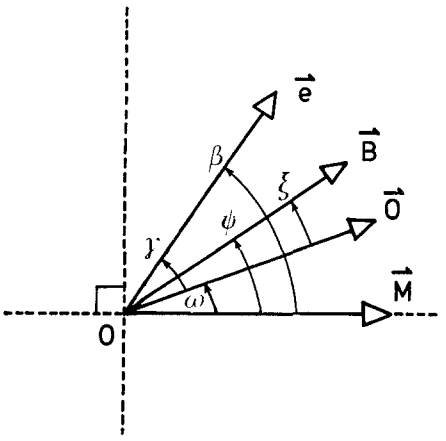

Fig. 7. Schematic of the angular relationships of the electric vectors of bleaching, (***B***), monitoring (***M***) and observed (**0**) beams to the projection (***e***) of the absorption/emission transition moment (***E***) of the probe onto the plane of the membrane (cf. Fig. 2)

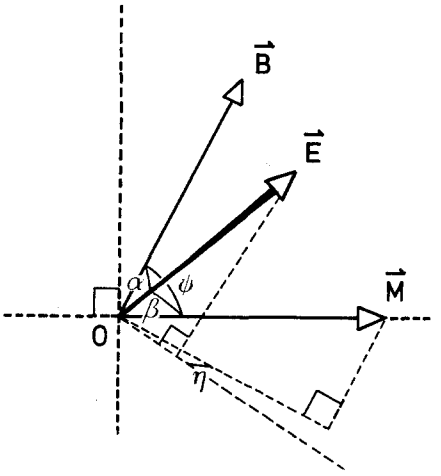

Fig. 8. Schematic of the angular relationships of the electric vectors of bleaching (***B***) and monitoring (***M***) beams to the probe absorption/emission transition moment vector (***E***). η is the dihedral angle between the projections of ***E*** and ***M*** onto the plane perpendicular to ***B***. The corresponding azimuth ϕ of ***E*** about ***B*** in the plane perpendicular to ***M***, also used in the text, is not shown

of the signal monitored after bleaching is given by:

$$I_\xi = C \sin^4\theta \int_{\beta=0}^{\pi} \{(2\cos^2\omega - 1)\,\overline{\cos^4\beta(t)} + 2\cos\omega\sin\omega\,\overline{\cos^3\beta(t)\sin\beta(t)} + \sin^2\omega\,\overline{\cos^2\beta(t)}\} \times \sum_{i=0}^{\infty} a_i(-B)^i \{(2\cos^2\psi - 1)\cos^2\beta + 2\cos\psi\sin\psi\cos\beta\sin\beta + \sin^2\psi\}^i\, d\beta\,, \quad (25)$$

where $\xi = \psi - \omega$, and $a_i = 1/i!$ or $1/(i+1)!$ for uniform and gaussian bleaching profiles respectively. Thus, in general, the evolution of a polarized component of the emission intensity, $I_\xi(t)$ will depend not only on $\overline{\cos^2\beta(t)}$ as does the unselected emission but also on the time-dependences $\overline{\cos^4\beta(t)}$ and $\overline{\cos^3\beta(t)\sin\beta(t)}$. Inspection of Eq. (25) reveals that these more complex time-dependences are eliminated only by simultaneously setting $\psi = 0$ or $\pi/2$ and $\omega = \cos^{-1}\sqrt{1/2} = \pi/4 = \omega_{m2}$ leading, after normalization by $I_\omega(-)$, to $F_\parallel(t)$ or $F_\perp(t)$, respectively. While the average of these two signals is free of rotational artifact [cf. Eq. (16)], there is no condition under which recovery (or depletion) in the FPR signal due to rotational diffusion may be eliminated when both bleaching and monitoring beams are polarized and a single polarized component of the emission is observed. It is also evident from Eq. (25), however, that abrogation of polarization selection either of the monitoring beam or, as assumed in examination of $F_\psi(t)$, in emission, also results in elimination of the higher order time-dependences, since their coefficients are now averaged out: $\langle\cos^2\omega\rangle = 1/2$, $\langle\cos\omega\sin\omega\rangle = 0$, and the results for $F_\psi(t)$ are all reproduced. If the bleaching beam is depolarized, on the other hand, there is no initial polarized photoselection, Eq. (25) effectively reduces, within a scale factor, to Eq. (23) and any polarized emission component, I_ω now, will be free of rotational artifact.

The 3-dimensional case

The relevant geometry for this situation (excluding a polarizer on the emission side) is pictured in Fig. 8. The before-bleach intensity of emission in all directions, is given by:

$$I(-) = C \int_{\phi=0}^{2\pi}\int_{\beta=0}^{\pi} \cos^2\beta\sin\beta\, d\beta\, d\phi = 4\pi C/3\,, \quad (26)$$

where ϕ is the azimuth of ***E*** in the plane normal to ***M***. The bleaching probabilities are of the same form as previously given in Eqs. (2) and (3), but with the bleaching parameter B related to the "unpolarized" bleaching parameter K by $K = B/3$ since now:

$$\langle\cos^2\alpha\rangle = \int_{\eta=0}^{2\pi}\int_{\alpha=0}^{\pi} \cos^2\alpha\sin\alpha\, d\alpha\, d\eta \Big/ \int_{\eta=0}^{2\pi}\int_{\alpha=0}^{\pi} \sin\alpha\, d\alpha\, d\eta = 1/3 \quad (27)$$

for random orientation in three dimensions. For a stationary situation, the after-bleach intensity is given by:

$$I_\psi = C \int_{\eta=0}^{2\pi}\int_{\alpha=0}^{\pi} \cos^2\beta\, P(B,\alpha)\sin\alpha\, d\alpha\, d\eta\,. \quad (28)$$

The normalized evolution of intensity with time after the δ-pulse bleach will depend, as in the 2-D case, on $\overline{\cos^2\beta(t)}$ which is given for the 3-D case by:

$$(3/2)\,\overline{\cos^2\beta(t)} - (1/2) = [(3/2)\cos^2\beta - (1/2)]\,f(t)\,, \tag{29}$$

where $f(t)$ is often a complex function, even for a single rotating species (see e.g. Ehrenberg and Rigler 1972) depending on the shape of the rotating unit, the orientation of the absorption/emission transition within it, and restriction of the angular range over which rotation may occur, e.g. for fluorophores embedded in a phospholipid vesicle membrane (Kinosita et al. 1977). The largest effects of concern here will be noted with unrestricted motion for which $f(t) \to 0$ as $t \to \infty$, the simplest case being that of a spherical rotor: $f(t) = \exp[-6D_r t]$, D_r being the isotropic rotational diffusion coefficient.

On combining Eqs. (26), (28) and (29), substituting for $\cos\beta$ according to the cosine rule:

$$\cos\beta = \cos\psi\cos\alpha + \sin\psi\sin\alpha\cos\eta \tag{30}$$

performing the integration over the azimuth η and collecting terms, the ratio of intensitities after and before bleaching may be expressed as:

$$\begin{aligned} F_\psi(t) &= [(3/2)\cos^2\psi - (1/2)]\,\{F(\infty) - F_\perp(0)\}\cdot f(t) \\ &\quad + F(\infty) \\ &= [(3/2)\cos^2\psi - (1/2)]\,\{F_\parallel(0) - F(\infty)\}\cdot f(t) \\ &\quad + F(\infty)\,, \end{aligned} \tag{31}$$

where:

$$F_\parallel(0) = \int_{\alpha=0}^{\pi/2} 3\cos^2\alpha\,P(B,\alpha)\sin\alpha\,d\alpha \tag{32}$$

$$F_\perp(0) = \int_{\alpha=0}^{\pi/2} (3/2)\sin^2\alpha\,P(B,\alpha)\sin\alpha\,d\alpha \tag{33}$$

and:

$$F(\infty) = \int_{\alpha=0}^{\pi/2} P(B,\alpha)\sin\alpha\,d\alpha\,. \tag{34}$$

Equation (11) with the above definitions (cf. Wegener and Rigler 1984) applies here as well as in the two-dimensional case, and again, the evolution of intensity after the flash can be expressed in terms of the (normal) emission anisotropy, defined for the three-dimensional case by:

$$\begin{aligned} r &= [F'_\parallel - F'_\perp]/[F'_\parallel + 2F'_\perp] = [F'_\parallel - F'_\perp]/3F'(\infty) \\ &= [F'_\parallel - F'(\infty)]/2F'(\infty) = [F'(\infty) - F'_\perp]/F'(\infty) \end{aligned} \tag{35}$$

leading to:

$$F_\psi(t) = F(\infty) - (3\cos^2\psi - 1)\,[1 - F(\infty)]\,r(t) \tag{36}$$

with:

$$r(t) = r_0\,f(t)\,. \tag{37}$$

Equation (36) is the equivalent in "F" form of Eq. (8) given by Wegener and Rigler (1984) in F' form. Again, the apparent laterally mobile fraction f_ψ^M defined in Eq. (21) is simply related to the emission anisotropy, e.g. for $\psi = 0$:

$$f_\parallel^M = 2r_0/(1 + 2r_0)\,. \tag{38}$$

The limits of r_0 for $B \to \infty$ and $B \to 0$ are 0 and 2/5 respectively leading to $0 \leqq f_\parallel^M \leqq 4/9$. The above results are summarised in Fig. 9 showing the dependence of $F_\psi(0)$ on B, Fig. 10 for $F_\parallel(0)$ and $F(\infty)$ as functions of B, Fig. 11 for f_ψ^M as a function of B, and Fig. 12 depicting the changes in $f_\parallel^M$ and r_0 with B.

It is further seen that, corresponding to Eq. (16) for the two-dimensional case:

$$F_{\psi_{m3}}(t) = F_{\psi_{m3}}(0) = [F_\parallel(0) + 2F_\perp(0)]/3 = F(\infty)\,, \tag{39}$$

where ψ_{m3} denotes the well-known "magic angle" for 3-D defined, as evident in Eqs. (31) and (36), by:

$$(3/2)\cos^2\psi_{m3} - (1/2) = 0; \quad \psi_{m3} = \cos^{-1}\sqrt{1/3} \simeq 55°. \tag{40}$$

As in the equivalent 2-D case, f_ψ^M disappears under this condition. Thus, in order to observe a total emission signal free of possible artifact introduced by rotational mobility, the bleaching and monitoring beam polarizations should be set at $\sim 55°$ to each other. This may be accomplished again by insertion of an appropriately rotatable polarizer or half-wave plate in the excitation beam path.

It should be noted, however, that in the usual microscope FPR configuration, even under the above conditions, the emission signal observed will not be proportional to the total emission, but will contain a component depending on $r(t)$, even if a depolarizing element is placed in the (in-line) observation path to obviate any instrumental bias. This is most easily seen by examining the effects of observing a particularly polarized component of the emission. Analogously to Eq. (23) for the 2-D case, the pre-bleach emission component polarized at an angle ω to the electric vector $\boldsymbol{M}$ of the monitoring beam is given by:

$$I_\omega(-) = C\int_{\eta=0}^{2\pi}\int_{\alpha=0}^{\pi} \cos^2\beta\cos^2\gamma\sin\alpha\,d\alpha\,d\eta\,, \tag{41}$$

where the cosine rule relates γ and ξ for the observation polarizer, corresponding to β and ψ for the monitoring polarizer, to α and η (cf. Eq. (30)]:

$$\cos\gamma = \cos\xi\cos\alpha + \sin\xi\sin\alpha\cos\eta \tag{43}$$

and (cf. Fig. 7):

$$\omega = \psi - \xi\,. \tag{43}$$

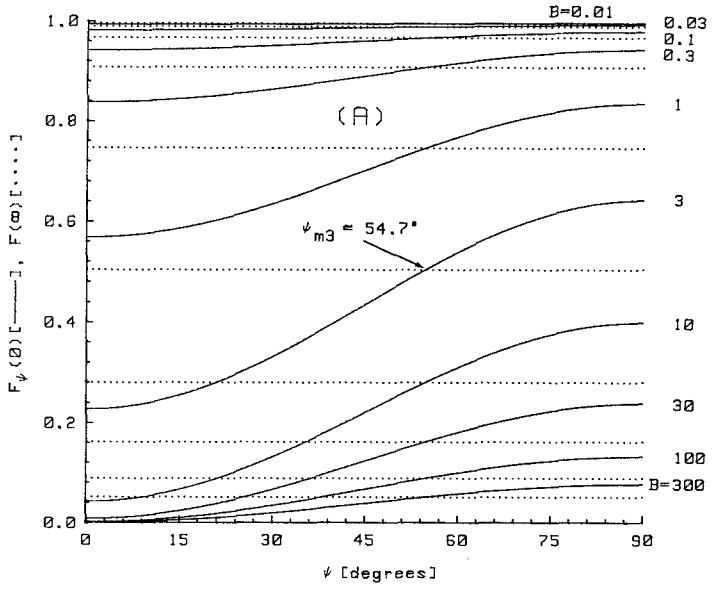

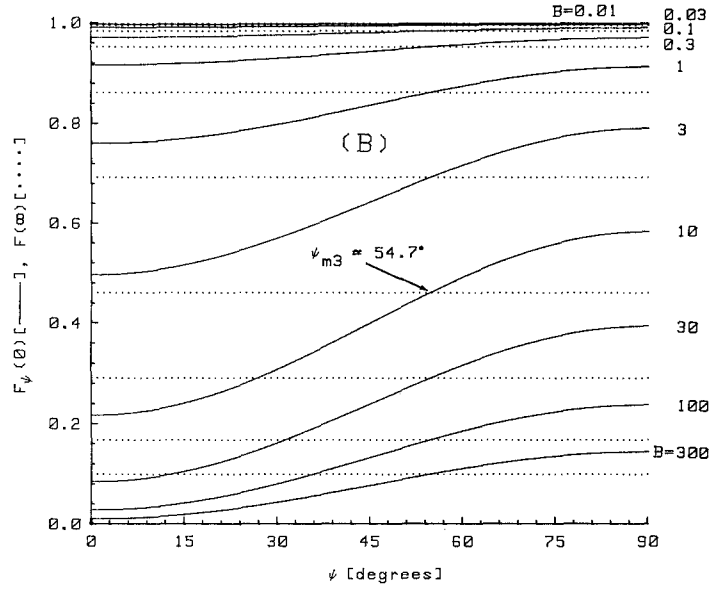

Fig. 9 A and B. As Fig. 3, but for 3-D (solution) FPR

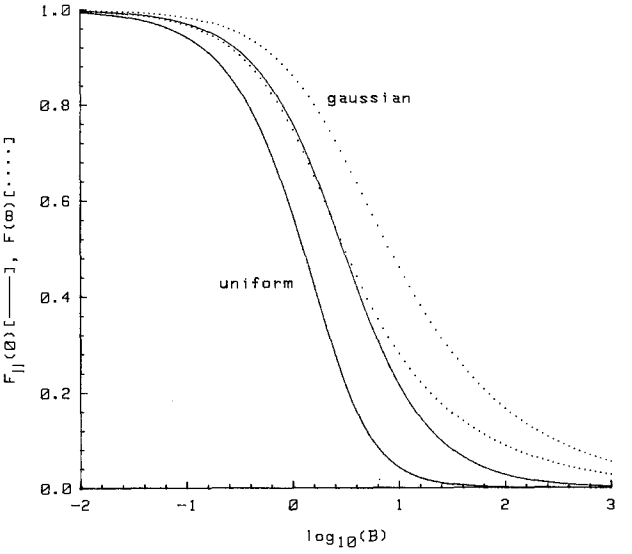

Fig. 10. As Fig. 4, but for 3-D (solution) FPR

On expanding the circular functions, integrating over η and α and collecting terms, the result reduces simply to:

$$I_\omega(-) = (4\pi C/15)\,[2\cos^2\omega + 1]. \tag{44}$$

Analogously to the 2-dimensional case [Eq. (25)], the time-dependence of intensity following the bleach may be written, changing from the above to the more convenient integration variables β and ϕ:

$$I_\xi(t) = C \int_{\phi=0}^{2\pi} \int_{\beta=0}^{\pi} \{(\cos^2\omega - \sin^2\omega\cos^2\phi)\,\overline{\cos^4\beta(t)}$$
$$+ 2\cos\omega\sin\omega\cos\phi\,\overline{\cos^3\beta(t)\sin\beta(t)}$$
$$+ \sin^2\omega\cos^2\phi\,\overline{\cos^2\beta(t)}\}\sum_{i=0}^{\infty} a_i(-B)^i \tag{45}$$
$$\cdot\{(\cos^2\psi - \sin^2\psi\cos^2\phi)\cos^2\beta$$
$$+ 2\cos\psi\sin\psi\cos\phi\cos\beta\sin\beta + \sin^2\psi\cos^2\phi\}^i\,d\beta\,d\phi.$$

The conditions for eliminating the higher order time-dependences are now more stringent than in the 2-dimensional case because of the effective appearance of the azimuth ϕ in $P(B,\alpha)$. Only for $\psi = 0$ and the 3-D "magic angle" condition $\omega = \cos^{-1}\sqrt{1/3} = \omega_{m3}$ will both higher order time-dependent rotational terms be eliminated, since only when ψ is zero will the coefficient of $\overline{\cos^4\beta(t)}$ contain the potentially "magic" factor $(3/2)\cos^2\omega - (1/2)$ after integration over the azimuth ϕ. Additionally, neither abrogation of polarization selection on the observation side nor depolarization of the bleaching and/or monitoring beams will provide any advantage in this respect, i.e. the depletion recovery equivalent to $F_\psi(t)$ defined in Eqs. (31) and (32) with $\psi = 0$ is the only signal observable in the in-line configuration considered that is free of higher order rotational correlation complexity. This results from the fact that part of the information content of the emission in the 3-D situation is not contained in components emitted "in-line" with the bleach/monitor beam but does appear in components perpendicular and at other angles to it. Thus, for the 3-dimensional case, it is necessary either to observe a signal or combination of signals proportional to the total emission collected over 4π (or, equivalently, 2π) steradians (Wegener and Rigler 1984), as expressed above in Eq. (39), or to monitor polarized "out-of-line" components (Wegener 1984) in order to free

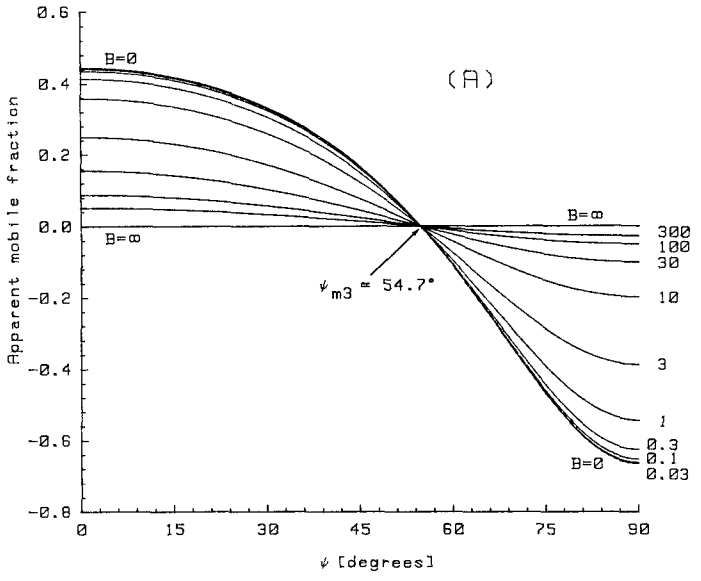

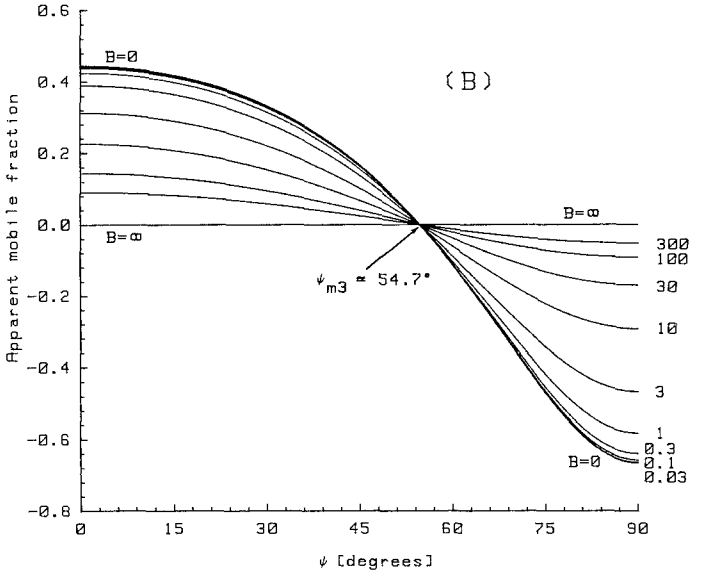

Fig. 11 A and B. As Fig. 5, but for 3-D (solution) FPR, and with depletion rather than recovery signals observed for $\cos^{-1}\sqrt{1/3} \simeq 55° < \psi \leqq \pi/2$

the recovery signal due to lateral diffusion from the effects of possible slow rotational diffusion.

Discussion

The above considerations demonstrate the existence of a considerable potential hazard in both the quantitative and qualitative interpretation of FPR data as generally obtained heretofore. As previously shown (Wegener and Rigler 1984; Wegener 1984), these cannot trivially be eliminated for 3-dimensional FPR (unoriented solution samples) in the usual in-line microscope configurations, but require

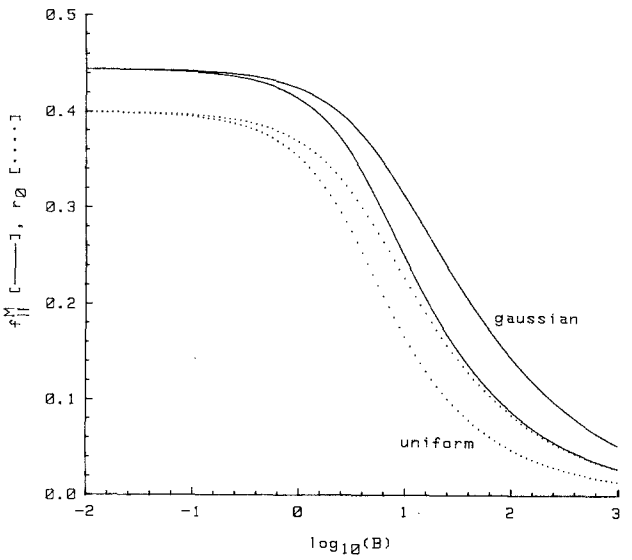

Fig. 12. As Fig. 6, but for 3-D (solution) FPR

hemispherical collection apertures and/or specialized rectangular or oblique geometries. On the other hand, they are rather simply eliminated for 2-dimensional FPR, in principle, by the additon of polarizing and/or depolarizing elements in the beam paths. In practice in the usual case, however, where a dichroic mirror is used to reflect the bleaching and monitoring beams through a right angle onto the sample and to select longer wavelength emission coming back along the same path from the sample, the partially polarizing properties of such a filter will further complicate the issue and render only the use of a properly oriented depolarizing element between it and the sample appropriate for complete elimination of these effects. The further addition of an appropriately reorientable polarizing element in the path of the laser beam before it is reflected from the dichroic mirror will still allow a polarized experiment to be performed in this arrangement.

Under the assumption of unbiased detection of emitted photons, the severity of the artifactual recovery (or depletion), induced by rotational relaxation has been maximised in the above by considering only the worst possible cases with respect to the optical parameters of the FPR apparatus and to other degrees of rotational freedom and photophysical parameters of the labelled diffusing species. In practice some, though not necessarily a great deal, of depolarization of the incoming laser beam, and considerable depolarization of the observed emission due to the rather high collection aperture of the microscope objective will occur, as discussed and quantitated by Smith et al. (1981b). The former effect is very simply dealt with in the 2-D case by considering the resultant $F_\psi(t)$ as the superposition

of signals originating from a combination of identically linearly polarized and unpolarized components of the bleaching and monitoring beams of polarization p_{ex} [defined as $(I_{max}-I_{min})/(I_{max}+I_{min})$, i.e. with reference to the beam itself rather than the laboratory coordinate system]. The "true" $p(t)$ in Eq. (17) may be replaced by the polarization which would be observed under this condition and which is given by $p_{obs}(t)=p_{ex}^2 p(t)$. Abrogation of rotational diffusion effects via the use of depolarized (or circularly polarized) excitation in the 2-D case follows directly from this relationship. Unfortunately, no such simple solution exists for the 3-D case, nor for emission aperture effects in either 2-D or 3-D (see Smith et al. 1981 b).

Factors associated with the fluorophore itself and, where appropriate, its attachment to a substrate rotating overall at rates comparable with the inverse time-scale of FPR observation, that will, possibly substantially, reduce the severity of the rotational artifact in lateral diffusion measurements by FPR, are:

(*a*) inherent non-coincidence of the absorption and emission transition moment vectors in the fluorophoric frame;

(*b*) torsional vibrations (Jabloński 1950) of the fluorophore over a restricted range occurring on a very fast time-scale ($\lesssim 0.1$ ns);

(*c*) limited fast time-scale ($\lesssim 1\,\mu s-1$ ms, depending on the system) rotational freedom of the fluorophore about the bond or bonds by which it may be attached to the rotating unit of primary interest;

(*d*) limited torsional or tumbling motions, on the same time-scale as in (*c*), of all or part of the rotating unit of primary concern in an, at least locally, anisotropic environment, superimposed on its main, long time-scale rotational relaxation, e.g. restricted torsion about or wobble of the axis (about which the "main" slow uniaxial rotation occurs) of a protein or subunit of a protein aggregate embedded in a phospholipid bilayer, local twisting and/or kinking of sub-units in an oligomer, polymer or aggregate with overall slow, unrestricted rotational freedom.

For the simplest cases considered here, namely, uniaxial rotation of a probe or labelled substrate in e.g. a planar membrane about the normal to that plane (2-D case), and isotropic rotation (or also special cases of anisotropic rotation in which the time-dependence of the anisotropy reduces to a monoexponential form) in solutions (3-D case), the diminution that is produced by the factors considered above of the extent of the possible rotational artifact in estimates of translational diffusion rates and immobile fractions by FPR measurements made without due regard to polarized photoselection effects, is rather simply taken into account, at least to a good first approximation. Taking the 3-dimensional case first, if the overall orientational distribution of the transition moments of the fluorophore is rapidly azimuthally randomized with respect to some axis in the overall rotating unit, the zero-point emission anisotropy r_0 whose magnitude determines the extent of the recovery (or depletion) artifact – see Eq. (36) et seq. and Eq. (29) et seq. – will be reduced from its limiting, B-dependent value by an overall depolarization factor d_3 which represents the product of the individual depolarization factors for each reorientational process (Soleillet 1929):

$$d_3=[(3/2)\cos^2\lambda-(1/2)]\prod_i[(3/2)\langle\cos^2\sigma_i\rangle-(1/2)], \tag{46}$$

where λ is the angle between absorption and emission transition moments in the fluorophore frame, while the average brackets denote (azimuthally random) averages over the distribution of polar angles σ_i characterising the i'th reorientational process. A more detailed discussion of this relationship and its limitations is given elsewhere in a different, but related context (Restall et al. 1984). In the case that the main relaxation process is not described by a monoexponential emission anisotropy decay, the factor in $\cos^2\lambda$ cannot be factorized out (see e.g. Wegener 1984), but the other depolarization processes may still be treated to a good approximation in this way. The occurrence of the 3-D magic angle condition in any one or more of these depolarizing processes ($\langle\cos^2\sigma_i\rangle=1/3$ corresponding to a very high degree of rotational freedom (2π or 4π steradians), or $\cos^2\lambda=1/3$) leads to immediate ablation of the rotational artifact in translational FPR in solution.

An analogous situation obtains in the 2-dimensional case. Here each depolarization factor is determined by the 2-D orientational distribution arising from projection of the physical 3-D distribution onto the sample plane. The overall depolarization factor d_2 multiplying the zero-point polarization p_0 – see Eqs. (17) and (20) et seq. – is given, analogously to Eq. (46), by:

$$d_2=(2\cos^2\zeta-1)\prod_i(2\langle\cos^2\varepsilon_i\rangle-1), \tag{47}$$

where ζ and ε_i are the projections of λ and σ_i onto the sample plane. Again, the appearance of the 2-D magic angle condition ($\langle\cos^2\varepsilon_i\rangle=1/2$, implying a very high degree of rotational freedom, or $\cos^2\zeta=1/2$) ablates the possible rotational artifact.

These depolarizing effects may well be quite extensive in many actual experimental cases and diminish the artifact to an undetectably low level. In addition, the size of aggregates in solution or in membrane systems, or the size of gel-phase patches

in an otherwise fluid liquid-crystalline membrane, that would rotate at rates sufficiently slow to induce the artifact, may actually be greater than the spot size or pattern period used in an FPR experiment. Under these conditions, the effect is lessened because only a part of the free isotropic or uniaxial rotation will be "seen" and contribute to the recovery (or depletion), i.e. the long-time limits of polarization or anisotropy, $p(\infty)$ and $r(\infty)$, assume non-zero values. A directed circular, spiral (whirlpool) or other curvilinear flow of membrane constituents, as opposed to random diffusion, would be expected to give rise to a similar effect.

In principle, the occurrence of a significant rotational artifact in FPR measurements of translational diffusion rates would be signalled by a smaller decrease in the immobile fraction on repeated bleaching than expected. If there is no rotational artifact present, then the immobile fraction will decrease geometrically with repeated bleachings of equal (less than unit) efficiency; at the other extreme, if all the recovery observed is rotational in origin (and no non-rotating species is present), the immobile fraction will remain constant from bleach to bleach. In the presence of both rotational and translational diffusion, however, this will surely be a difficult, if not impossible, diagnostic. A cleaner alternative would be to record FPR curves at different "spot" sizes (or pattern periodicities): the retention of a component of the decay having a constant exponential time-dependence would indicate its rotational origin. In the limit of large illumination area, *only* this component would effectively remain.

The most straightforward test in principle of the presence of rotational diffusion, however, is to compare $F_{\parallel}(t)$ and $F_{\perp}(t)$ either directly or by forming the polarization or anisotropy decay function from them for enhanced sensitivity, after incorporating appropriate polarizing and depolarizing elements into the beam paths as indicated earlier in the discussion. Such a system, including appropriate collection geometry for the 3-D case, has the obvious advantage that, not only can translational diffusion processes be definitively freed from any possible rotational interference, but any rotational motion on the appropriate time-scale (although, as already pointed out, it cannot be directly monitored free of interference from translational diffusion on the same time-scale which will contribute to depolarization by exchanging the orientationally selected unbleached fluorophore population for an unselected one) can be quantitated and exploited to aid in providing a better insight into the nature and complexity of such structured and heterogeneous two- and three-dimensional systems as, for example, the plasma membrane and cytoplasmic compartment of living cells. The modifications to existing FPR apparatus required to accomplish this for the oriented membrane case at least, would appear to be inexpensive and relatively trivial to commission.

Acknowledgements. This work was supported by the Cancer Research Campaign. The author is indebted to Drs. J. P. Keene and E. J. Land for essential discussion on bleaching kinetics.

Appendix

Expansions of $F_{\parallel}(0)$ and $F(\infty)$ for small values of the bleaching parameter B

In the evaluation of Eqs. (10), (13), (32) and (34), for $F_{\parallel}(0)$ and $F(\infty)$ from which $F_{\psi}(0)$, f_{ψ}^{M} and p_0 may all be derived, direct evaluation of the exponentials in $P(B, \alpha)$ was not accurate enough for small values of B. For this reason, and also for speed of calculation, all the functions presented in Figs. 3–6 and 9–12 were actually calculated up to $B = 1$ as the analytical integrals of the expansions up to fifth order terms in B. The expansions are all of the form:

$$F = \sum_{i=0}^{\infty} (-1)^i q_i B^i \qquad \text{(A1)}$$

and the coefficients q_i ($i = [0,5]$) are given in Table 1.

Table 1. Coefficients q_i in the integrated expansions of $F_{\parallel}(0)$ and $F(\infty)$ up to 5th order

Dimension	Beam profile	Component	q_0	q_1	q_2	q_3	q_4	q_5
2-D	uniform	$F_{\parallel}(0)$	1	3/4	5/16	35/384	21/1,024	77/20,480
		$F(\infty)$	1	1/2	3/16	5/96	35/3,072	21/10,240
	gaussian	$F_{\parallel}(0)$	1	3/8	5/48	35/1,536	21/5,120	77/122,880
		$F(\infty)$	1	1/4	1/16	5/384	7/3,072	7/20,480
3-D	uniform	$F_{\parallel}(0)$	1	3/5	3/14	1/18	1/88	1/520
		$F(\infty)$	1	1/3	1/10	1/42	1/216	1/1,320
	gaussian	$F_{\parallel}(0)$	1	3/10	1/14	1/72	1/440	1/3,120
		$F(\infty)$	1	1/6	1/30	1/168	1/1,080	1/7,920

References

Aizenbud AL, Gershon ND (1982) Diffusion of molecules on biological membranes of non-planar form. Biophys J 38:287–293

Axelrod D (1985) Fluorescence photobleaching techniques and lateral diffusion. In: Bayley PM, Dale RE (eds) Spectroscopy and the dynamics of molecular biological systems. Academic Press, New York, pp 163–176

Axelrod D, Koppel DE, Schlessinger J, Elson E, Webb WW (1976) Mobility measurement by analysis of fluorescence photobleaching recovery kinetics. Biophys J 16:1055–1069

Barisas BG (1984) Photobleaching recovery studies of the mobility of polymeric antigens on B cell surfaces. In: Perelson AS, DeLisi C, Wiegel FW (eds) Cell surface dynamics. Concepts and models. Marcel Dekker, New York, pp 167–202

Bretscher MS (1980) Lateral diffusion in eukaryotic cell membranes. Trends Biochem Sci (TIBS) 5(10): VI–VII

Dale RE (1985) Interpretation of fluorescence photobleaching recovery experiments on oriented cell membranes. FEBS Lett 192:255–258

Edidin M (1981) Molecular motions and membrane organization and function. In: Finean JB, Michell RH (eds) Membrane structure. Elsevier/North Holland, Amsterdam, pp 37–82

Edidin M, Zagyansky Y, Lardner TJ (1976) Measurement of membrane protein lateral diffusion in single cells. Science 191:466–468

Ehrenberg M, Rigler R (1972) Polarized fluorescence and rotational brownian motion. Chem Phys Lett 14:539–544

Elson HF, Yguerabide J (1979) Membrane dynamics of differentiating cultured embryonic chick skeletal muscle cells by fluorescence microscopy techniques. J Supramol Struct 12:47–61

Flanagan MT (1980) More light on membrane protein mobility. Nature 284:126

Hoffman W, Restall CJ (1983) Rotational and lateral diffusion of membrane proteins as determined by laser techniques. In: Chapman D (ed) Biomembrane structure and function. Macmillan Press, London, pp 257–318

Hughes BD, Pailthorpe BA, White LR (1981) The translational and rotational drag on a cylinder moving in a membrane. J Fluid Mech 110:349–372

Hughes BD, Pailthorpe BA, White LR, Sawyer WH (1982) Extraction of membrane microviscosity from translational and rotational diffusion coefficients. Biophys J 37:673–676

Jabloński A (1950) Fundamental polarization of photoluminescence and torsional vibrations of molecules. Acta Phys Pol 10:193–206

Jabloński A (1960) On the notion of emission anisotropy. Bull Acad Pol Sci Ser Sci Math Astron Phys 8:259–264

Jacobson K (1980) Fluorescence recovery after photobleaching: lateral mobility of lipids and proteins in model membranes and on single cell surfaces. In: Hillenkamp F, Pratesi R, Sacchi CA (eds) Lasers in biology and medicine. Plenum Press, New York, pp 271–288

Jacobson K (1983) Lateral diffusion in membranes. Cell Motility 3:367–373

Jacobson K, Wojcieszyn J (1981) On the factors determining the lateral mobility of cell surface components. Comments Mol Cell Biophys 1:189–199

Jacobson K, Derzko Z, Wu E-S, Hou Y, Poste G (1976a) Measurement of the lateral mobility of cell surface components in single living cells by fluorescence recovery after photobleaching. J Supramol Struct 5:565–576

Jacobson K, Wu E, Poste G (1976b) Measurement of the translational mobility of concanavalin A in glycerol-saline solutions and on the cell surface by fluorescence recovery after photobleaching. Biochim Biophys Acta 433:215–222

Jacobson K, Elson E, Koppel D, Webb W (1982) Fluorescence photobleaching in cell biology. Nature 295:283–284

Johnson P, Garland PB (1981) Depolarization of fluorescence depletion. FEBS Lett 132:252–256

Kaprelyants AS (1985) Lateral non-homogeneity and lateral diffusion of proteins in membranes. Trends Biochem Sci (TIBS) 10:385–386

Kell DB (1984) Diffusion of protein complexes in prokaryotic membranes: fast, free, random or directed? Trends Biochem Sci (TIBS) 9:86–88; ibid 379

Kinosita K Jr, Kawato S, Ikegami A (1977) A theory of fluorescence polarization decay in membranes. Biophys J 20:289–305

Koppel DE (1979) Fluorescence redistribution after photobleaching. A new multipoint analysis of membrane translational dynamics. Biophys J 28:281–291

Koppel DE (1983) Fluorescence photobleaching as a probe of translational and rotational motions. In: Sha'afi RI, Fernandez SM (eds) Fast methods in physical biochemistry and cell biology. Elsevier, New York, pp 339–367

Koppel DE, Axelrod D, Schlessinger J, Elson EL, Webb WW (1976) Dynamics of fluorescence marker concentration as a probe of mobility. Biophys J 16:1315–1329

Lessing HE, von Jena A (1976) Separation of rotational diffusion and level kinetics in transient absorption spectroscopy. Chem Phys Lett 42:213–217

Lessing HE, von Jena A (1979) Continuous picosecond spectroscopy of dyes. In: Stich ML (ed) Laser handbook. North-Holland, Amsterdam, pp 753–846

Lessing HE, von Jena A, Reichert M (1975) Orientational aspect of transient absorption in solutions. Chem Phys Lett 36:517–522

O'Shea PS (1984) Lateral diffusion: the archipelago effect. Trends Biochem Sci (TIBS) 9:378

O'Shea PS (1985) 2-D diffusion and the structure of biological membranes. Trends Biochem Sci (TIBS) 10:231

Owicki JC, McConnell HM (1980) Lateral diffusion in inhomogeneous membranes. Model membranes containing cholesterol. Biophys J 30:383–398

Peters R (1981) Translational diffusion in the plasma membrane of single cells as studied by fluorescence microphotolysis. Cell Biol Int Rep 5:733–760

Peters R, Cherry RJ (1982) Lateral and rotational diffusion of bacteriorhodopsin in lipid bilayers: experimental test of the Saffman-Delbrück equations. Proc Natl Acad Sci USA 79:4317–4321

Peters R, Peters J, Tews KH, Bähr W (1974) A microfluorimetric study of translational diffusion in erythrocyte membranes. Biochim Biophys Acta 367:282–294

Pink DA (1985) Constraints on protein lateral diffusion. Trends Biochem Sci (TIBS) 10:230

Restall CJ, Dale RE, Murray EK, Gilbert CW, Chapman D (1984) Rotational diffusion of calcium-dependent adenosine-5′-triphosphatase in sarcoplasmic reticulum: a detailed study. Biochemistry 23:6765–6776

Saffman PG (1976) Brownian motion in thin sheets of viscous fluid. J Fluid Mech 73:593–602

Saffman PG, Delbrück M (1975) Brownian motion in biological membranes. Proc Natl Acad Sci USA 72:3111–3113

Schlessinger J, Koppel DE, Axelrod D, Jacobson K, Webb WW, Elson EL (1976) Lateral transport on cell membranes: mobility of concanavalin A receptors on myoblasts. Proc Natl Acad Sci USA 73:2409–2413

Singer SJ, Nicolson GL (1972) The fluid mosaic model of the structure of cell membranes. Science 175:720–731

Smith BA, McConnell HM (1978) Determination of molecular motion in membranes using periodic pattern photobleaching. Proc Natl Acad Sci USA 75:2759–2763

Smith BA, Clark WR, McConnell HM (1979) Anisotropic molecular motion on cell surfaces. Proc Natl Acad Sci USA 76:5641–5644

Smith LM, McConnell HM, Smith BA, Parce JW (1981a) Pattern photobleaching of fluorescent lipid vesicles using polarized laser light. Biophys J 33:139–146

Smith LM, Weis RM, McConnell HM (1981b) Measurement of rotational motion in membranes using fluorescence recovery after photobleaching. Biophys J 36:73–91

Soleillet P (1929) Sur les paramètres, caractérisant la polarisation partielle de la lumière dans les phénomènes de fluorescence. Ann Phys (Paris) 12:23–97

Tait JF, Frieden C (1982) Polymerization and gelation of actin studied by fluorescence photobleaching recovery. Biochemistry 21:3666–3674

van Zoelen EJJ, Tertoolen LGL, de Laat SW (1983) Simple computer method for evaluation of lateral diffusion coefficients from fluorescence photobleaching recovery kinetics. Biophys J 42:103–108

Vaz WLC, Hallmann D (1983) Experimental evidence against the applicability of the Saffman-Delbrück model to the translational diffusion of lipids in phosphatidylcholine bilayer membranes. FEBS Lett 152:287–290

Vaz WLC, Derzko ZI, Jacobson KA (1982) Photobleaching measurements of the lateral diffusion of lipids and proteins in artificial phospholipid bilayer membranes. In: Poste G, Nicolson GL (eds) Membrane reconstitution. Elsevier, New York, pp 83–136

Vaz WLC, Goodsaid-Zalduondo F, Jacobson K (1984) Lateral diffusion of lipids and proteins in bilayer membranes. FEBS Lett 174:199–207

Vaz WLC, Clegg RM, Hallmann D (1985) Translational diffusion of lipids in liquid crystalline phase phosphatidylcholine multibilayers. A comparison of experiment with theory. Biochemistry 24:781–786

Ware BR (1985) Dynamic light scattering and fluorescence photobleaching recovery: application of complementary techniques to cytoplasmic mobility. In: Bayley PM, Dale RE (eds) Spectroscopy and the dynamics of molecular biological systems. Academic Press, New York, pp 133–161

Webb WW (1981) Luminescence measurements of macromolecular mobility. Ann NY Acad Sci 366:300–314

Weber G (1953) Rotational brownian motion and polarization of the fluorescence of solutions. Adv Protein Chem 8:415–459

Wegener WA (1984) Fluorescence recovery spectroscopy as a probe of slow rotational motions. Biophys J 46:795–803

Wegener WA, Rigler R (1984) Separation of translational and rotational contributions in solution studies using fluorescence photobleaching recovery. Biophys J 46:787–793

Wolf DE, Handyside AH, Edidin M (1982) Effect of microvilli on lateral diffusion measurements made by the fluorescence photobleaching recovery technique. Biophys J 38:295–297

Yguerabide J (1971) Quoted in Reference (19) of Elson and Yguerabide (1979)

Zagyansky Y, Edidin M (1976) Lateral diffusion of concanavalin A receptors in the plasma membrane of mouse fibroblasts. Biochim Biophys Acta 433:209–214